Relationship between macromolecular network and fatigue properties of unfilled polychloroprene rubber

Pierre-Yves Le Gac[a,*], Pierre-Antoine Albouy[b], Bruno Fayolle[c], Jacques Verdu[c]

[a] IFREMER Centre de Bretagne, Marine Structures Laboratory, BP70, 29280 Plouzané, France
[b] Laboratoire de Physique des Solides, CNRS, Université Paris-Sud, Université Paris-Saclay, 91405 Orsay, France
[c] PIMM, Arts et Metiers Institute of Technology, CNRS, Cnam, HESAM University, 151 boulevard de l'Hopital, 75013 Paris, France

A B S T R A C T

Fatigue life of unfilled polychloroprene rubber is characterized in fully relaxing ($R = 0$) and non-relaxing conditions ($R = 0.2$) for more than 15 network structures. Network changes are induced by thermal oxidation ageing of the rubber and characterized especially in terms of crosslink density. For the first time, in the case of unfilled elastomers, we show that an increase in crosslink density leads to a decrease in fatigue life, which cannot be attributed to large changes in strain-induced crystallization processes. The results obtained here are used to determine the relationship between network structure and fatigue properties. In fully relaxing conditions, it is possible to predict fatigue lifetime by considering crosslink density using a theoretical energetic approach. Nevertheless, the same approach does not work in non-relaxing conditions. In the latter case, a new empirical relationship is proposed to link fatigue life to the crosslink density of rubber.

1. Introduction

Elastomers are macromolecular materials with a relatively low crosslinking density and a glass transition temperature that is lower than their normal temperature of use. These characteristics explain their substantial stretching ability and their low stiffness. They have the capacity to undergo repeated mechanical cycling of large amplitude, usually known as fatigue resistance. Furthermore, it is well known that elastomers such as the polydienes family are sensitive to chemical ageing, in particular to oxidation, which limits its lifetime in use condition.

This fatigue resistance of rubbers is not yet fully understood, which can be explained by the fact that this scientific area is still quite new compared to metals, for instance. Indeed, the first significant publication dedicated to elastomer fatigue was published in 1940 [1], whereas the first major work on metals was published in 1847 by Wöhler, that is, almost a century prior.

The majority of works on elastomer fatigue published in the last 80 years use an experimental approach, most frequently in relation to natural rubber due to its extensive range of applications [2-6]. It has been highlighted that the fatigue life (defined here as the number of cycles before breakage) of rubbers largely depends on a range of parameters such as mechanical loading conditions [7-9]. For given test conditions, the fatigue life of rubber also depends on the nature of the gum [10-11] and the additives used for the formulation (fillers and stabilizers [12-13], process conditions, and as expected, ageing of the material before testing [14-16]). From the existing studies, if it clearly emerges that the nature of the macromolecular network is one of the key parameters when considering the fatigue behavior of rubber [17-19], the network properties of an elastomer have not yet been successfully linked to its fatigue life [20].

As a result, we propose in this study to investigate the influence of macromolecular modifications induced by oxidation, the final purpose here is to relate chemical ageing and fatigue properties which is poorly documented in the literature to our knowledge [15,16] even non-existent in the case of neoprene.

We chose here to modify a polychloroprene network by oxidative ageing, which allows us to assess a large number of different networks over a wide range of crosslink densities. It is well known that during the oxidation of chloroprene rubber, crosslink density increases through radical reactions on the double bonds of the polymer backbone that leads to an increase in rubber stiffness [21,22]. This increase in crosslink density leads to substantial changes in mechanical properties such as higher modulus, decreased elongation at break, and lower crack propagation energy under static loading [23-26]. Considering in a first approach that the crosslinking density is a key parameter determining the mechanical properties, our objective here is to study the possi-

Table 1.
Detailed formulation for the polychloroprene rubber used in this study.

CR (W type)	100 phr
MgO	4 phr
ZnO	5 phr
Sulfur	1.5 phr
Stearic Acid	0.5 phr
HPPD	3 phr

ble relationships between the fatigue behavior and the changes in crosslinking density induced by oxidation

It is known that polychloroprene rubbers (CR), like natural rubber, undergoes strain-induced crystallization (SIC) when stretched [27,28]. This phenomenon has been widely studied [20,29-33], confirming that it drastically reduces the crack propagation rate due to the formation of crystallites at the crack tip (where the local strain is the largest). This results in a large increase in the fatigue life of rubbers. This is especially true when crystallites formed during stretching do not melt during unloading, and in this case, there is a cumulative effect. One of the simplest ways to avoid the melting of crystallites is to ensure that fatigue occurs with a positive loading ratio R, where R is classically defined as the ratio between the minimum and maximum strain with rubbers [8]. In this study, both $R = 0$ and $R = 0.2$ testing conditions will be considered to emphasize the role of SIC on CR fatigue properties as a function of network properties.

This paper will begin by presenting the formulation of the unaged material and the experimental methods. The impact of oxidation-induced changes in crosslink density on the mechanical properties is then investigated; this includes elastic modulus, elongation at break, and fatigue life under different loading conditions. These results are discussed in the third part of the paper in light of existing theoretical considerations, and formulas linking network properties and fatigue life are proposed for this class of CR.

2. Material and methods

2.1. Material

Samples are made based on the classic formulation provided in Table 1. The starting gum is a homopolymer (W-type) whose exact microstructure is assesed using nuclear magnetic resonance: trans-1,4 (91.8%), cis-1,4 (6%), 1,2-units (1.5%), and 3,4-units (0.7%). Crosslinking is obtained by sulfur vulcanization carried out at 160 °C for 10 min in a custom-made compression mould.

2.2. Ageing

Network changes are induced by the thermal oxidation of samples in Memmert ovens at ageing temperatures of 80 °C, 95 °C, and 110 °C. In these conditions, oxidation is not spatially limited by oxygen diffusion, and samples have a homogeneous degradation level through thickness [34].

2.3. Soluble fraction

The soluble fraction is measured according to ISO1817 [35] using toluene as solvent. Results presented here are averaged over three samples of the same batch.

2.4. Tensile test

Tensile tests are performed on dogbone samples (type 3 in ISO37 standard [36]) with a 50 N load cell, and the applied strain

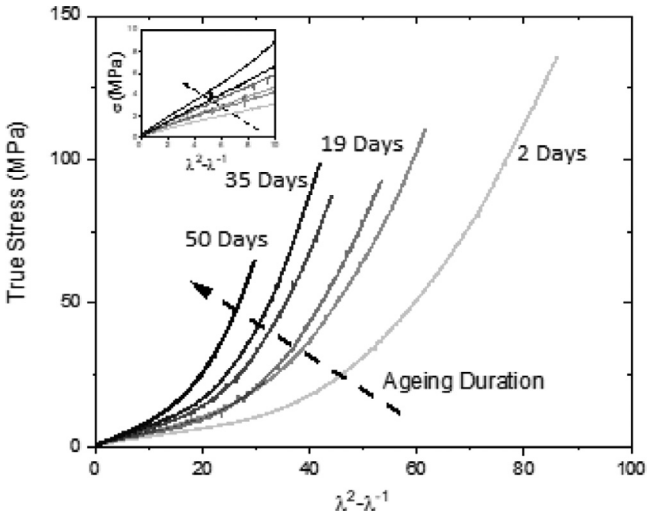

Fig. 1.. Changes in tensile behavior of unfilled polychloroprene during oxidation at 80 °C.

is measured using digital image correlation. As above, results are averaged over three samples of the same batch.

2.5. Fatigue test

Actual fatigue tests are performed on custom-built electrically driven machines (actuators Parker PRA 3810S). The testing machines apply a sinusoidal displacement-controlled loading, and the minimum and maximum positions are assessed either visually or with a linear variable differential transformer sensor. Tests are performed in air at room temperature with loading ratios of $R = 0$ and $R = 0.2$ and different maximum extensions. Let us recall that the loading ratio R is the strain ratio at minimum and maximum extension. All fatigue experiments are performed at 2.0 Hz, and the lifetime is determined as the time at sample total failure; seven samples are tested for each test, and the results are averaged. The maximum local stretch ratio differs from the prescribed global stretch ratio due to sample geometry. Here, the local stretch ratio is measured by digital image correlation (DIC) using a high-speed camera. More details about the testing procedure and machine can be found in [37].

2.5. In-situ RX testing

To characterize strain-induced crystallization, a specific device is used. The apparatus, which is described in detail in [29], is a symmetric stretching machine mounted on a rotating anode generator; the K_α radiation emitted by the copper anode is selected by a doubly curved graphite monochromator providing high flux (ca. 5 10^9 ph/s when operated at 40 kV, 40 mA). The set-up is equipped with a hybrid pixel detector. From X Ray pattern, it is possible to define and measure crystallinity index (CI) as the ratio of the area under the crystallization peaks to the total scan area.

3. Results

This section presents the experimental results relating to the macromolecular network, tensile behavior, and lastly, fatigue behavior changes. First, we will focus on the results obtained with samples aged at 80 °C to describe the processes involved. Second, the results obtained at other ageing temperatures will be presented in order to build a master curve for a given reference temperature.

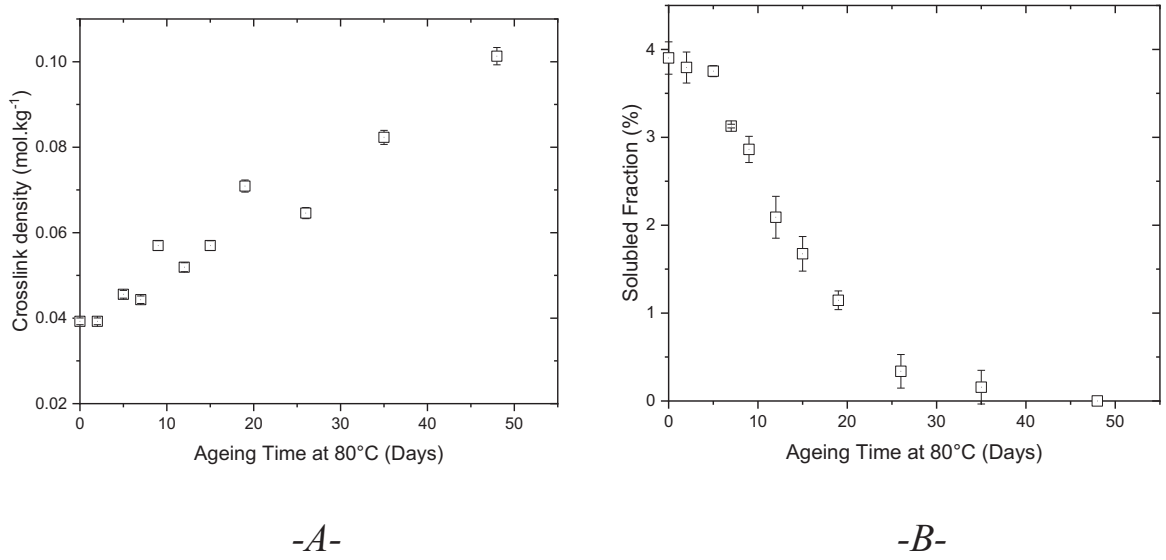

Fig. 2.. Changes in the polychloroprene network induced by oxidation, with an increase in crosslink density (A) and a decrease in soluble fraction (B).

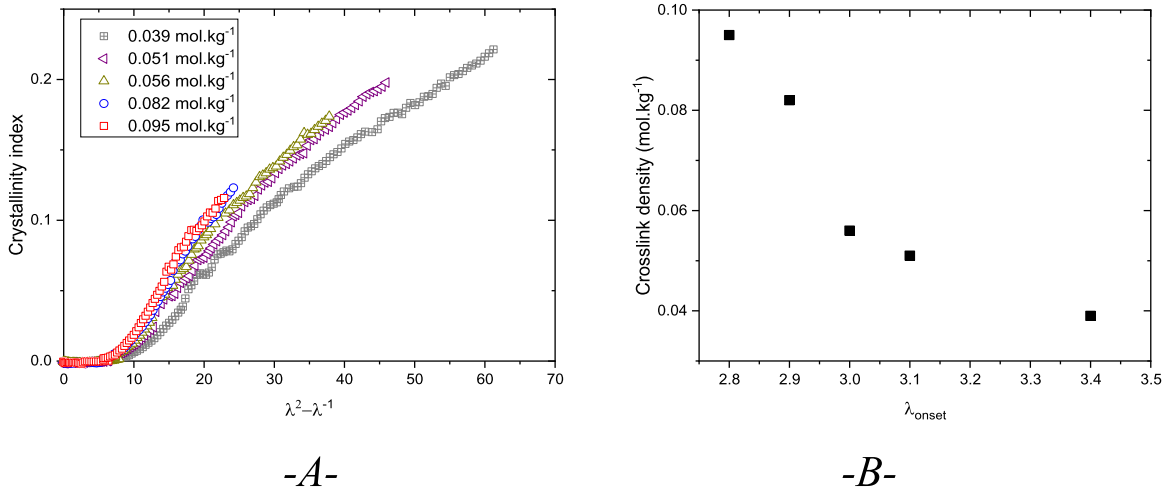

Fig. 3.. Crystallinity index measured during in-situ traction tests for several crosslink densities (A) lonset as function of crosslink density (B).

3.1. Effect of oxidation on tensile properties

We first focus on the changes induced by an oxidation at 80 °C. As seen in Fig. 1, oxidation results in an increase in stiffness (see insert in Fig. 1) and a decrease in ultimate properties. The modulus increases results from the increase in crosslink density induced by the oxidative attack of double bonds located on the polymer backbone, as commonly observed in most polydiene elastomers.

In Fig. 2-A, we plot the crosslink density deduced from the value of the elastic modulus at small deformations (see insert, Fig. 1) based on the classical theory of rubber elasticity where $E = 3.\rho.\mathrm{RT}.\nu$ (with E is the modulus, ρ the polymer density and ν the crosslink density). We also observe a strong decrease in the soluble fraction (see Fig. 2-B), and both effects are in accordance with existing knowledge available in the literature for CR [21-23].

SIC is known to play an important role with mechanical properties, and the effect of the oxidation-driven increase in crosslink density on the crystallinity index is shown in Fig. 3. The main impact of this increase in crosslink density is a slight decrease in the elongation at crystallization onset (λ_{onset}) from $\lambda_{Onset} \approx 3.4$ for the pristine sample (0.039 mol.kg^{-1}) to $\lambda_{Onset} \approx 2.8$ for a sample aged for 50 days (0.095 mol.kg^{-1}), Fig. 3B. This result can be put in parallel with the case of natural rubber, where crosslink density changes only weakly affect λ_{onset} [30]. This result is at variance with the classical SIC theory developed by Flory, which predicts a strong effect of the crosslink density on λ_{onset}. To date, this discrepancy has not been explained.

3.2. Fatigue behavior of the unaged network

The number of cycles (N) to failure for the unaged network is plotted in Fig. 4 as a function of the maximum elongation imposed during the fatigue test (λ_{max}) for two cases. We first consider the case where the ratio between minimum and maximum strain, R, is set to zero ("fully relaxing conditions"); as expected, an increase in maximum extension leads to a decrease in fatigue life. For $\lambda_{max} = 3.5$, crystallites are grown during extension but completely disappear during full relaxation [29,33]. In the second case where $R = 0.2$, mean fatigue life is strongly improved by a factor that reaches ca.100 for $\lambda_{max} = 2.5$. In such "non-relaxing conditions," it may be assumed that crystallites grown during extension do not fully melt during retraction. Indeed, crystallite melting occurs at an extension slightly above 1 for CR [29].

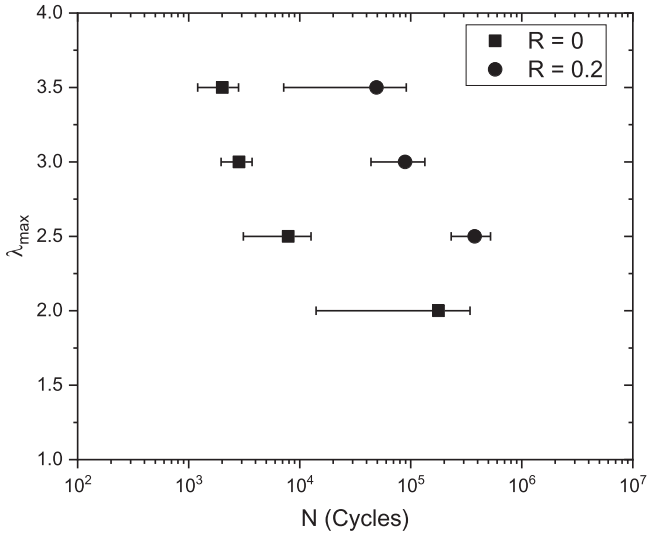

Fig. 4.. Number of cycles to failure as a function of maximum elongation for unaged CR in relaxing ($R = 0$) and non-relaxing conditions ($R = 0.2$).

3.3. Fatigue lifetime as a function of oxidation state

The number of cycles to failure as a function of ageing time in unfilled CR in both relaxing ($R = 0$, $\lambda_{max} = 2.5$) and non-relaxing conditions ($R = 0.2$, λ_{max}=2) is given in Fig. 5. Although an increase in fatigue life is witnessed for $R = 0.2$ with short ageing times (i.e., less than 3 days of exposure), it appears that the crosslinking process during oxidation at 80 °C mainly leads to a gradual decrease in fatigue life in both relaxing and non-relaxing conditions. The overall decay in the number of cycles is significantly more pronounced in non-relaxing conditions (10^6 to 10^3 cycles) compared to relaxing conditions (10^4 to 10^3 cycles). Although the physical origin of the slight increase at the beginning of ageing still seems unclear, the general trend for the fatigue life decay is strongly associated with the crosslinking process. As for the unaged samples, this decay is interpreted in terms of the melting or non-melting of SIC-grown crystallites, with the SIC-grown mechanism being disadvantaged by the crosslinking.

A decrease in fatigue properties during ageing has already been reported in the literature for filled natural rubber [14-16] but never for CR.

3.4. Effect of ageing temperatures

To consider the link between the macromolecular network and fatigue properties from a general perspective, and thus avoid any specificity induced by ageing at 80 °C, two other ageing temperatures are considered: 95 °C and 110 °C. Obviously, an increase in ageing temperature leads to an increase in the degradation kinetic, but our main concern here is to generate several networks using the oxidation degradation. In the framework of time-temperature superposition usually used for ageing purposes, we thus used a normalized ageing time with a shift factor (a_T) that depends on ageing temperature (Fig. 6). a_T shows an apparent activation energy close to 70 kJ/mol for all properties.

The same behavior is observed for all ageing conditions considered here (Fig. 6): increase in crosslink density, decrease in strain at break, and decrease in fatigue life. Based on the results presented in this section, it will be possible to discuss the relationships between mechanical properties and crosslink density; this is the aim of the next section.

4. Discussion

This section focuses on establishing a relationship between the crosslink density of the macromolecular network and the failure properties during the fatigue test for both R-factors studied here. Two approaches can be followed here:

i) The first way is based on the relationship proposed by Lake [38] to link the number of cycles at failure (N) to λ_{max} using the strain energy function. In this approach, it is considered that fatigue refers to failure due to the growth of some initial crack under cyclic loading. The cyclic crack growth rate mainly relates to the maximum tearing energy (G) attained during loading.

ii) A second way is to test possible correlations between crosslinking density, elongation at break in static loading (λb), and the number of cycles at failure, while assuming several relationships associated with the rubber elasticity theory.

4.1. Energetic approach

According to Lake [38], the cyclic crack growth rate dc/dn is related in intermediate tearing energy region to the maximum tearing energy (G) by the following power law:

$$\frac{dc}{dn} = BG^{\beta} \tag{1}$$

This leads to Eq. (2) for the number of cycles at break N with the assumption that fatigue tests are performed on a sample without an initial hand-made cut. We call c_0 the intrinsic flaw size.

$$N = \frac{1}{(\beta - 1)B(2KW)^{\beta} c_o^{\beta-1}} \tag{2}$$

Here the strain energy density W is related to G by $G = 2KW$. Factor K depends on the maximum extension λ_{max} through $K = \pi/\sqrt{\lambda_{max}}$. B and β are the material properties related to crack propagation [20].

According to the classical theory of rubber elasticity, the strain energy density is related to λ_{max} by Eq. (3) [39,40]:

$$W = \rho RT\nu(\lambda_{max} + 2/\lambda_{max} - 3)/2 \tag{3}$$

where ρ is the polymer density and ν the crosslink density.

To establish a relationship between fatigue life and crosslink density (and hence ageing time), a two-step approach is used for both $R = 0$ and $R = 0.2$ conditions:

- Parameters β and B introduced in Eq. (2) are first identified based on the results obtained with the pristine starting material tested at several strain levels λ_{max} (i.e., different strain energies).

- Eqs (2) and 3 are combined in a second step to predict the fatigue life of rubber of known crosslink density, considering that β and B parameters are not largely affected by network changes.

We first focus on the fully relaxing condition ($R = 0$). Fig. 7 presents the number of cycles before failure as a function of the inverse of strain energy for unaged samples tested at four strain levels (data from Fig. 3). A value of 4.4 is found for β, significantly higher than values reported in the literature for Natural Rubber (NR), although this value is in accordance with the physical considerations previously made for rubber fatigue [15]. The value of B has been calculated considering initial flaw size (c_o) of 0.1 mm [15].

Using β and B determined with unaged sample, a prediction of the fatigue life is proposed in Fig. 8. During ageing, the increase in crosslink density leads to an increase in the strain energy density (if the mechanical loading remains the same, here $\lambda_{max} = 2$) and so a decrease in fatigue life at the sample. Based on Fig. 8 it appears a simple relationship exists between fatigue

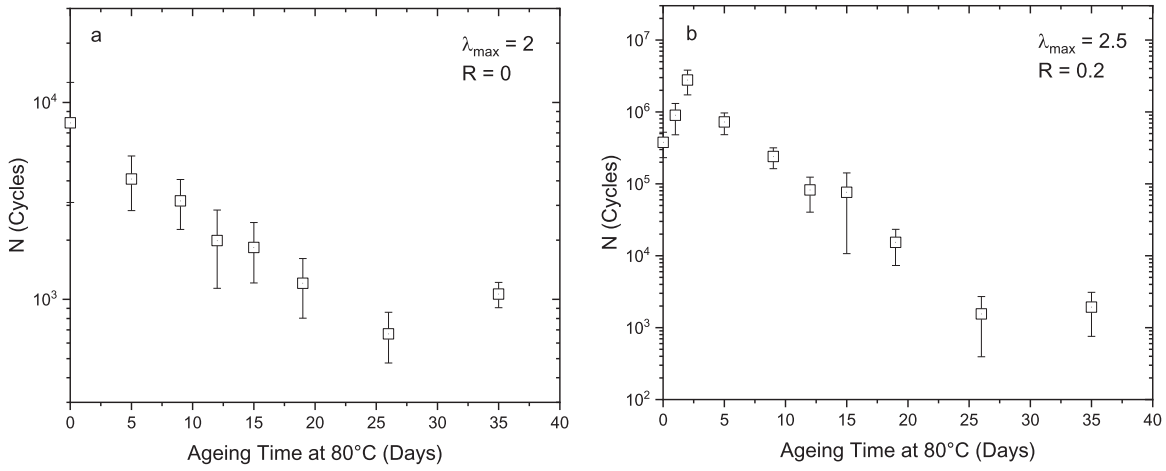

Fig. 5.. Number of cycles to failure as a function of ageing time in unfilled CR in relaxing (A) ($R = 0$, l_{max}=2, a) and non-relaxing conditions (B) ($R = 0.2$, l_{max}=2.5).

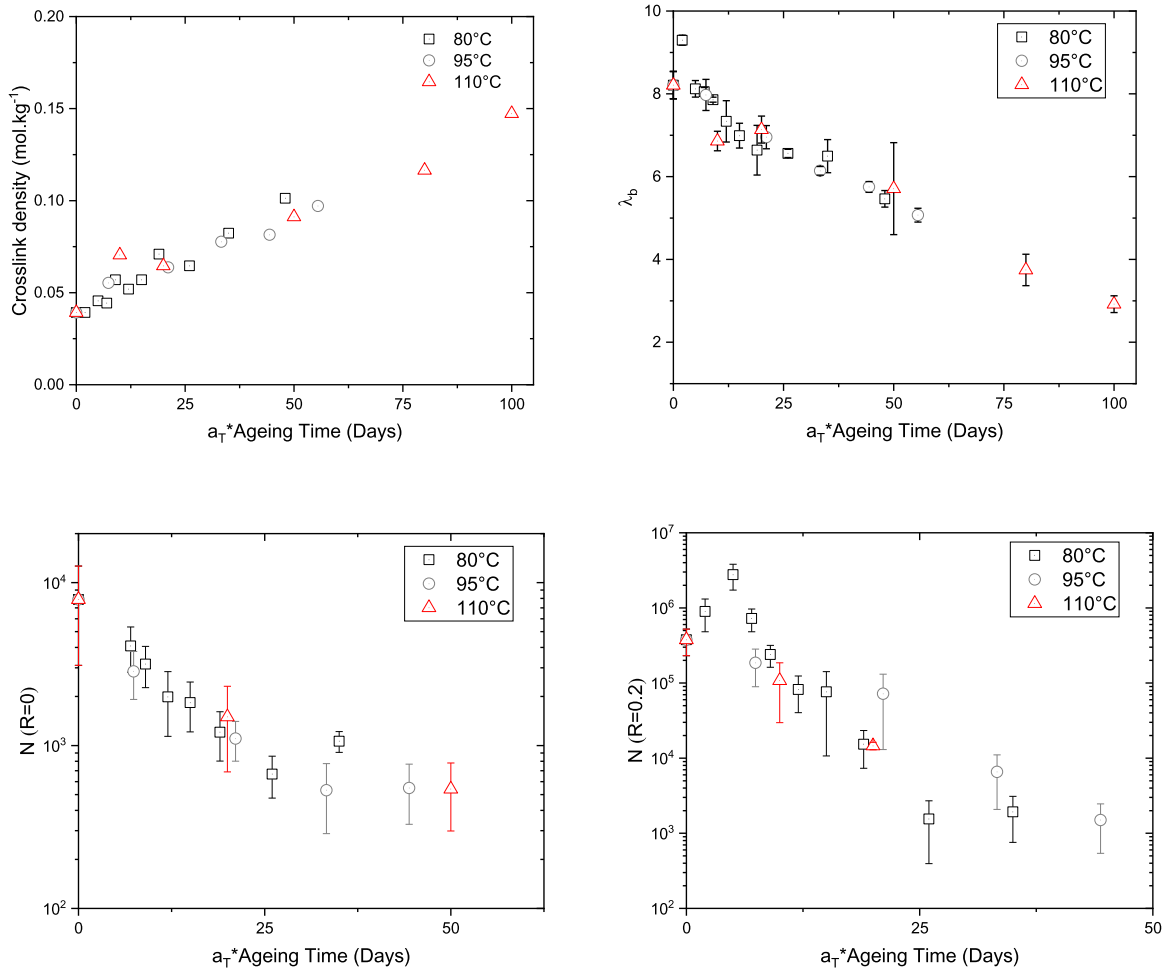

Fig. 6.. Crosslink density (A), elongation at break (B), as well as fatigue life in relaxing conditions (C) and non-relaxing conditions (D) as a function of ageing time.

life and crosslink density of unfilled rubber in fully relaxing conditions. To the best of our knowledge, this has never before been demonstrated for CR.

The same approach is now applied to the fatigue life of CR in non-relaxing conditions where SIC is expected to play a more important role. Fig. 9-A presents the number of cycles to failure as function of strain energy for the unaged sample with $R = 0.2$. The β value is equal to 3.8 compared to 4.4 in the fully relaxing condition; it thus remains in the same range. The value of B is much lower when $R = 0.2$ compared to $R = 0$ due to the fact that the fatigue life of CR is enhanced when $R>0$. These results are compared to data obtained from thermally aged CR samples in Fig. 9-B with the following marked disagreements being observed. This means that it is not possible to propose a prediction of fatigue life in non relaxing condition of CR. First, at lower ageing times (higher values for $1/2KW$), N is higher than the predicted value , which is directly

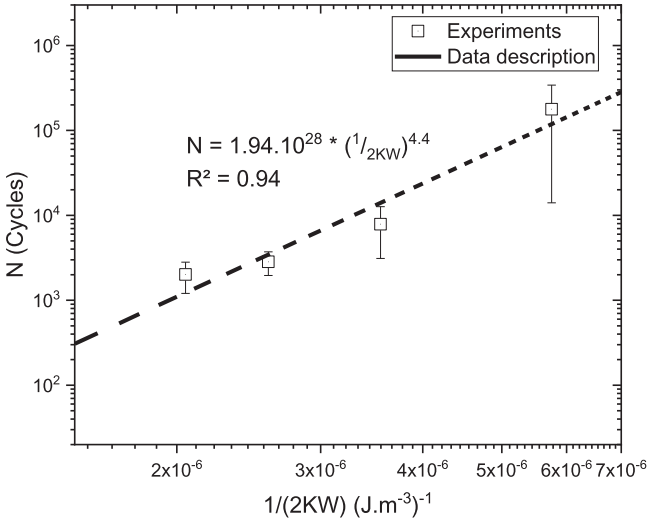

Fig. 7.. Identification of b and B with the unaged sample in relaxing conditions. The strain energy variation is induced by a change in maximum extension.

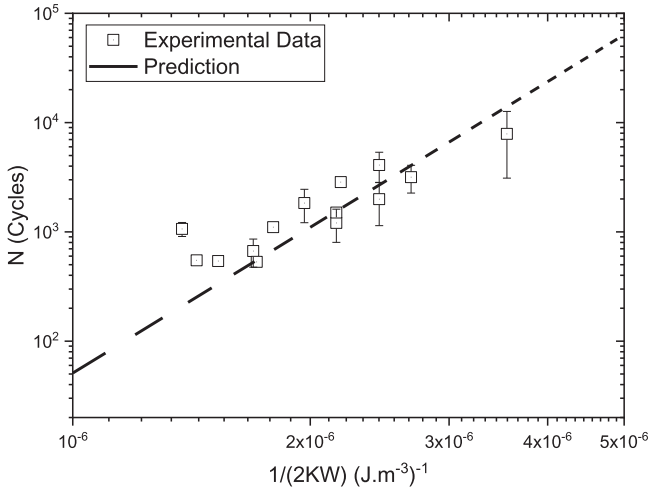

Fig. 8.. Relationship between the fatigue life of unfilled chloroprene rubber and crosslink density (through strain energy) with $R = 0$ and maximum extension 2. The strain energy variation is induced by a change in crosslink density (ageing time).

related to the increase in N reported above for shorter ageing times ; as already mentioned, the origin of this effect is not known. Second, N is lower than predicted at higher ageing times (lower values for $1/2KW$). We reported above that SIC starts at a lower extension with an increasing ageing time; the overall SIC process should thus be favored. A positive impact on fatigue life could therefore be expected contrary to what is observed. However , it is known that SIC is accompanied by a highly significant relaxation of the no n-crystallized fraction . In other words, the strain energy density W should be affected. To go further on the origin of the behavior, it would be necessary to perform crack propagation measurements with the different networks.

4.2. Correlation between fatigue life and crosslink density

No reliable relationship between fatigue life and crosslink density in non-relaxing conditions can be obtained based on the previous theoretical considerations. We therefore propose investigating a possible empirical relation. First, it is interesting to verify the existence of a possible correlation between fatigue life (N) and elongation at break in quasistatic conditions (λ_b) for all networks (aged and unaged) as proposed in the literature. In Fig. 10, we plotted the number of cycles N to failure for a given maximum elongation ($\lambda_{max} = 2$) in both relaxing ($R = 0$) and non-relaxing ($R = 0.2$) conditions as a function of elongation at break, λ_b. A linear relationship is clearly observed in both relaxing and non-relaxing conditions.

In rubbers, two basic mechanisms can be considered for breakdown: the formation and growth of cavities in the matrix or a cooperative rupture of interconnected and highly loaded network chains. The second mechanism has been observed for unfilled rubber, and elongation at break λ_b can be related to the maximum extensibility of a network; it is recalled below how the latter can be estimated using the classical theory of rubber elasticity [40]. We thus call N_e the average number of monomers of length l per chain and C_∞ the characteristic ratio that defines the number of monomers per statistical segment. The length of the fully extended chain is $R_{max} = N_e l$, and the mean-square distance of both ends in the quiescent state is $\langle R^2 \rangle = N_e C_\infty l^2$. An estimate of the maximum extension ratio λ_m is thus:

$$\lambda_m \sim R_{max}/\sqrt{\langle R^2 \rangle} = \sqrt{N_e/C_\infty} \tag{4}$$

Real networks are inhomogeneous, and it can be hypothesized that the local extension of some chains in parts of the sample reaches λ_m at a lower applied macroscopic extension. Rupture occurs at this point that defines elongation at break λ_b. It is thus expected that λ_b displays a similar dependence on crosslink density ν as λ_m, ie

$$\lambda_b \sim \sqrt{N_e} \sim \nu^{-1/2} \tag{5}$$

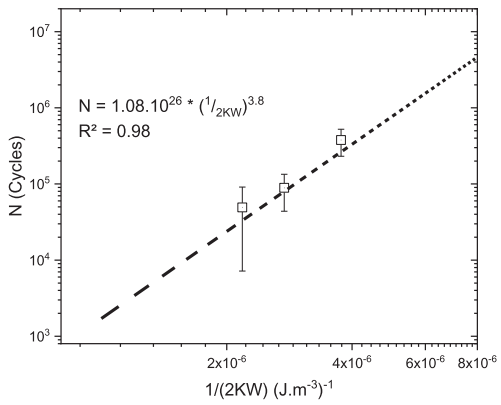

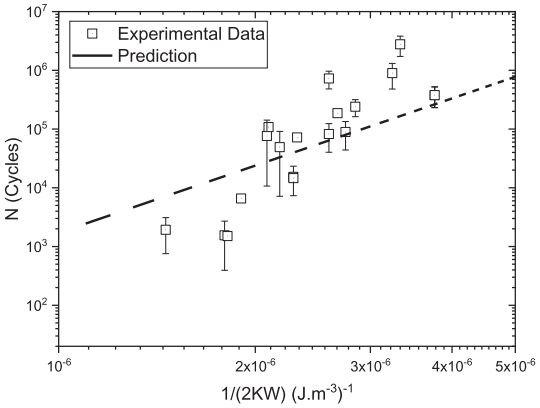

Fig. 9.. Determination of b and B using unaged samples (A) and prediction of fatigue life as a function of the inverse of strain energy directly related to crosslink density (B) with $R = 0.2$.

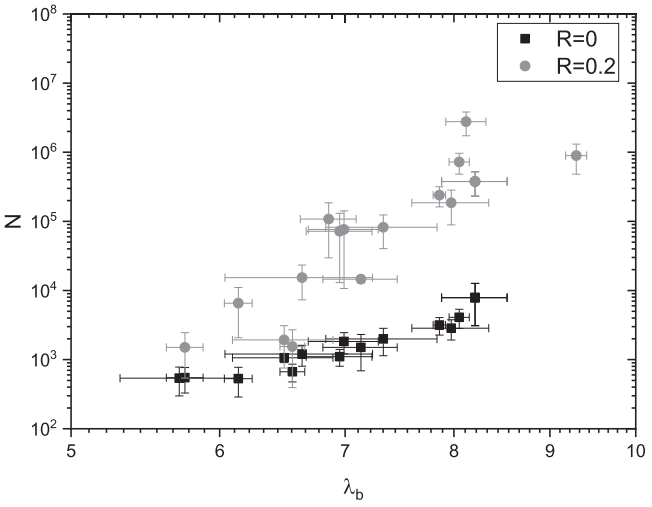

Fig. 10.. Relationship between elongation at break and maximum number of cycles at $R = 0$ and $R = 0.2$ in log/log scale for all aged and unaged networks.

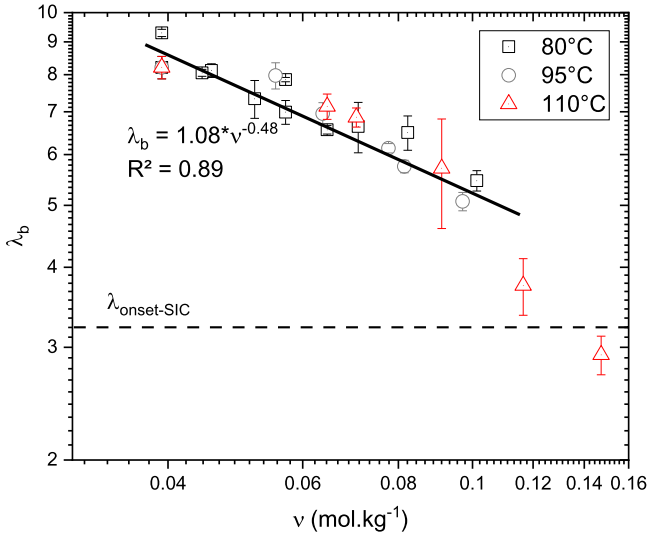

Fig. 11.. Relationship between elongation at break measured during the tensile test and crosslink density in polychloroprene rubber.

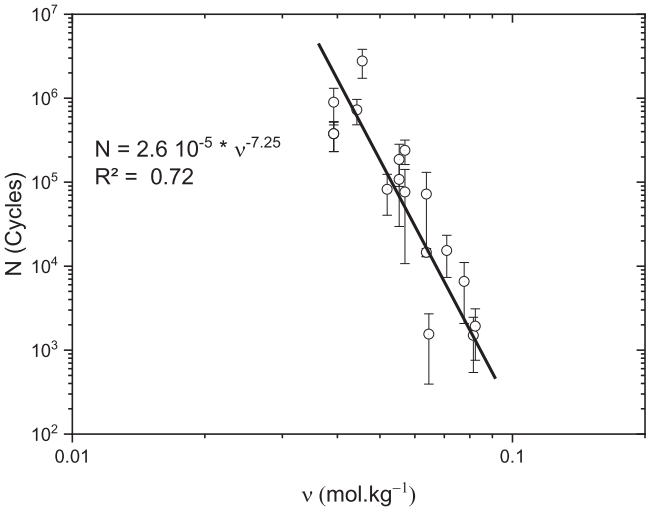

Fig. 12.. Empirical relationship between the fatigue life of unfilled polychloroprene rubber and crosslink density when tested in non-relaxing conditions ($R = 0.2$).

Fig. 9 presents elongation at break as a function of crosslink density in a log/log scale. Except for the two points that correspond to maximum elongation close to the elongation at SIC onset, a slope of −0.5 is actually observed. This is clear evidence that in static conditions, the failure of unfilled CR is related to the maximum extension of chains.

Let us now consider dynamic loading. By combining Figs. 10 and 11, it is possible to relate fatigue life (N) to crosslinking density under non-relaxed conditions. Fig. 12 shows the existence of a scale law between these two quantities. The exponent of this scaling law is of the order of 7 here, although the physical meaning of this value needs further investigation.

5. Conclusions

Network changes in unfilled CR can be induced by thermal oxidation, which leads to an increase in crosslink density evidenced by an increase in stiffness. This also results in a pronounced decrease in elongation at break. Based on the classical theory of rubber elasticity, it is possible to propose relationships between strain at break and crosslink density.

The strain-induced crystallization process is very important for the mechanical behavior of rubbers with both quasistatic and dynamic properties. Based on this work, we can conclude that this process is not markedly affected by the increase in crosslink density, which only results in a slight decrease in elongation at the onset of crystallization.

Considering fatigue properties, it clearly emerges that an increase in crosslink density leads to a large decrease in the fatigue life of unfilled rubber. This behavior occurs in both fully relaxing ($R = 0$) and non-relaxing conditions ($R = 0.2$).

Drawing on existing theory, a relationship between the fatigue life of unfilled CR and crosslink density has been highlighted for the first time when $R = 0$. It may therefore be of interest to generalize it to other rubbers or formulations. In non-relaxing conditions where SIC plays a more important role than in fully relaxing conditions, the same approach was used, but it was not possible to describe the decrease in fatigue life based on the estimated strain energy alone. The exact origin of this behavior will need further investigation. However, an alternative empirical relationship is proposed for these non-relaxing conditions.

Declaration of Competing Interest

The authors whose names are listed immediately below certify that they have NO affiliations with or involvement in any organization or entity with any financial interest (such as honoraria; educational grants; participation in speakers' bureaus; membership, employment, consultancies, stock ownership, or other equity interest; and expert testimony or patent-licensing arrangements), or non-financial interest (such as personal or professional relationships, affiliations, knowledge or beliefs) in the subject matter or materials discussed in this manuscript.

References

[1] S.M. A Cadwell, R.A. Merrill, C.M. Sloman, F.L. Yost, Dynamic fatigue life of rubber, Rubber Chem. Technol. 13 (2) (1940) 304–315.

[2] K. Brüning, K. Schneider, S.V. Roth, G. Heinrich, Strain-induced crystallization around a crack tip in natural rubber under dynamic load, Polymer (Guildf) 54 (22) (2013) 6200–6205.

[3] S. Kaang, C. Nah, Fatigue crack growth of double-networked natural rubber, Polymer (Guildf) 39 (11) (1998) 2209–2214.

[4] G.M. Bartenev, F.A. Galil-Ogly, Dynamic fatigue of rubber and the mechanism of failure by repeated deformations, Rubber Chem. Technol. 29 (2) (1956) 504–508.

[5] G.J. Lake, P.B. Lindley, Cut growth and fatigue of rubbers. II. Experiments on a noncrystallizing rubber, J. Appl. Polym. Sci. 8 (2) (1964) 707–721.

[6] G.J. Lake, P.B. Lindley, Mechanical fatigue limit for rubber, Rubber Chem. Technol. 39 (2) (1966) 348–364.

[7] A.G. Thomas, Rupture of rubber. V. Cut growth in natural rubber vulcanizates, J. Polym. Sci. 31 (123) (1958) 467–480.
[8] W.V. Mars, A. Fatemi, Factors that affect the fatigue life of rubber: a literature survey, Rubber Chem. Technol. 77 (3) (2004) 391–412.
[9] O. Gehrmann, N.H. Kröger, A. Muhr, Displacement-controlled fatigue testing of rubber is not strain-controlled, Int. J. Fatigue 145 (2021) 106083.
[10] Engineering with RubberHow to Design Rubber Components, A. Gent (Ed.), Carl Hanser Verlag, Munich, 1992 ch. 2.
[11] C.M. Roland, Network recovery from uniaxial extension: I. Elastic equilibrium, Rubber Chem. Technol. 62 (5) (1989) 863–879.
[12] A.A. Katbab, G. Scott, Mechanisms of antioxidant action: the involvement of nitroxyl radicals in the antifatigue action of secondary amines, Eur. Polym. J. 17 (5) (1981) 559–565.
[13] P.Y. Le Gac, M. Arhant, P. Davies, A Muhr, Fatigue behavior of natural rubber in marine environment: comparison between air and sea water, Mater. Des. 65 (2015) 462–467 1980-2015.
[14] C. Neuhaus, A. Lion, M. Johlitz, P. Heuler, M. Barkhoff, F. Duisen, Fatigue behaviour of an elastomer under consideration of ageing effects, Int. J. Fatigue 104 (2017) 72–80.
[15] P.H. Mott, C.M. Roland, Aging of natural rubber in air and seawater, Rubber Chem. Technol. 74 (1) (2001) 79–88.
[16] M. Broudin, Y. Marco, V. Le Saux, P. Charrier, W. Hervouet, P.Y. Le Gac, Investigation of thermo-oxidative ageing effects on the fatigue design of automotive anti-vibration parts, MATEC Web of Conferences, 165, EDP Sciences, 2018 No. 08004.
[17] L.C. Yanyo, Effect of crosslink type on the fracture of natural rubber vulcanizates, in: Structural Integrity, Springer, Dordrecht, 1989, pp. 103–110.
[18] S.G. Kim, S.H. Lee, Effect of crosslink structures on the fatigue crack growth behavior of NR vulcanizates with various aging conditions, Rubber Chem. Technol. 67 (4) (1994) 649–661.
[19] G.R. Hamed, Effect of crosslink density on the critical flaw size of a simple elastomer, Rubber Chem. Technol. 56 (1) (1983) 244–251.
[20] Chazeau, L., Chenal, J.M., Gauthier, C., Kallungal, J., & Caillard, J. (2020). About the Influence of Materials Parameters on the Ultimate and Fatigue Properties of Elastomers. Fatigue Crack Growth in Rubber Materials: Experiments and Modelling, 297-329.
[21] F. Delor, J. Lacoste, J. Lemaire, N. Barrois-Oudin, C. Cardinet, Photo-and thermal ageing of polychloroprene: effect of carbon black and crosslinking, Polym. Degrad. Stab. 53 (3) (1996) 361–369.
[22] P.Y. Le Gac, G. Roux, J. Verdu, P. Davies, B Fayolle, Oxidation of unvulcanized, unstabilized polychloroprene: a kinetic study, Polym. Degrad. Stab. 109 (2014) 175–183.
[23] P.Y. Le Gac, M. Celina, G. Roux, J. Verdu, P. Davies, B Fayolle, Predictive ageing of elastomers: oxidation driven modulus changes for polychloroprene, Polym. Degrad. Stab. 130 (2016) 348–355.
[24] P.Y. Le Gac, M. Broudin, G. Roux, J. Verdu, P. Davies, B Fayolle, Role of strain induced crystallization and oxidative crosslinking in fracture properties of rubbers, Polymer (Guildf) 55 (10) (2014) 2535–2542.
[25] T. Ha-Anh, T. Vu-Khanh, Prediction of mechanical properties of polychloroprene during thermo-oxidative aging, Polym. Test. 24 (6) (2005) 775–780.
[26] R. Bouaziz, L. Truffault, R. Borisov, C. Ovalle, L. Laiarinandrasana, G. Miquelard–Garnier, B. Fayolle, Elastic properties of polychloroprene rubbers in tension and compression during ageing, Polymers (Basel) 12 (10) (2020) 2354.
[27] P.Y. Le Gac, P.A. Albouy, D Petermann, Strain-induced crystallization in an unfilled polychloroprene rubber: kinetics and mechanical cycling, Polymer (Guildf) 142 (2018) 209–217.
[28] P. Zhang, G. Huang, L. Qu, Y. Nie, G. Weng, J. Wu, Strain-induced crystallization behavior of polychloroprene rubber, J. Appl. Polym. Sci. 121 (1) (2011) 37–42.
[29] P.Y. Le Gac, P.A. Albouy, P Sotta, Strain-induced crystallization in a carbon-black filled polychloroprene rubber: kinetics and mechanical cycling, Polymer (Guildf) 173 (2019) 158–165.
[30] J.M. Chenal, L. Chazeau, L. Guy, Y. Bomal, C. Gauthier, Molecular weight between physical entanglements in natural rubber: a critical parameter during strain-induced crystallization, Polymer (Guildf) 48 (4) (2007) 1042–1046.
[31] Z.T. Xie, M.C. Luo, C. Huang, L.Y. Wei, Y.H. Liu, X. Fu, J. Wu, Effects of graphene oxide on the strain-induced crystallization and mechanical properties of natural rubber crosslinked by different vulcanization systems, Polymer (Guildf) 151 (2018) 279–286.
[32] P.A. Albouy, A. Vieyres, R. Pérez-Aparicio, O. Sanséau, P. Sotta, The impact of strain-induced crystallization on strain during mechanical cycling of cross-linked natural rubber, Polymer (Guildf) 55 (16) (2014) 4022–4031.
[33] B. Huneau, Strain-induced crystallization of natural rubber: a review of x-ray diffraction investigations, Rubber Chem. Technol. 84 (3) (2011) 425–452.
[34] M. Celina, J. Wise, D.K. Ottesen, K.T. Gillen, R.L. Clough, Correlation of chemical and mechanical property changes during oxidative degradation of neoprene, Polym. Degrad. Stab. 68 (2) (2000) 171–184.
[35] ISO1817
[36] ISO37
[37] K.N. Ulu, B. Huneau, P.Y. Le Gac, E. Verron, Fatigue resistance of natural rubber in seawater with comparison to air, Int. J. Fatigue 88 (2016) 247–256.
[38] G.J. Lake, Fatigue and fracture of elastomers, Rubber Chem. Technol. 68 (3) (1995) 435–460.
[39] A.N. Gent, P.B. Lindley, A.G. Thomas, Cut growth and fatigue of rubbers. I. The relationship between cut growth and fatigue, J. Appl. Polym. Sci. 8 (1) (1964) 455–466.
[40] Treloar, L.R.G. (1975). The physics of rubber elasticity.